

Window Functions And Time-Domain Plotting In HFSS And SIwave

Greg Pitner

Introduction

HFSS and SIwave allow for time-domain plotting of S-parameters. Often, this feature is used to calculate a step response or time-domain reflectometry (TDR) plot of the structure being simulated. Fourier analysis provides the mathematical mechanism for transforming frequency sweep data to a time-domain plot, but two approximations are involved. First, the transform is between two sets of discrete data points, as opposed to continuous waveforms. Second, the frequency sweep data cannot have infinite bandwidth, but must truncate at some upper limit. This note will discuss the implications of these approximations, and provide information for successful time-domain plotting.

Transforming Frequency- To Time-Domain

It is easier to make generalizations about the effect of finite bandwidth if we have continuous functions. Consequently, we will initially assume our frequency- and time-domain data is continuous, and defer discussion of the effects of discretization until later. With a continuous-time sweep over an infinite bandwidth, we could – at least in principle – calculate a time-domain response by multiplying our sweep data $S(f)$ with the spectrum of a time-domain excitation function $E(f)$ and evaluating the inverse Fourier integral¹:

$$f(t) = \int_{-\infty}^{\infty} S(f)E(f)e^{2\pi jft} df$$

In practice, however, sweep data does not extend to infinite frequencies and is restricted to a bandwidth b . If we simply assume that the spectrum is zero-valued outside of the bandwidth, we can interpret the data as an infinite sweep that has been multiplied by a rectangular “window” function $W(f)$, with a value of 1 within the bandwidth and a value of 0 otherwise.

$$f(t) = \int_{-\infty}^{\infty} W(f)S(f)E(f)e^{2\pi jft} df = \int_{-b}^b S(f)E(f)e^{2\pi jft} df$$

This process is illustrated in Fig. 1, assuming that $S(f)E(f)$ corresponds to an ideal unit step function in the time domain. In Fig 1.a, the frequency spectrum is truncated beyond a certain upper limit. Since multiplication in the frequency domain corresponds to convolution in the time domain, this has the effect of convolving the time-domain step with a sinc function – the inverse Fourier transform of the rectangle (Fig 1.b). The final result is an edge with a finite rise time and some oscillation.

¹ Frequency sweep data consists only of positive frequencies, but the negative frequencies are simply the complex conjugate of the positive: $S(-f) = S^*(f)$. This is true for any frequency-domain function when the corresponding time-domain waveform is real-valued.

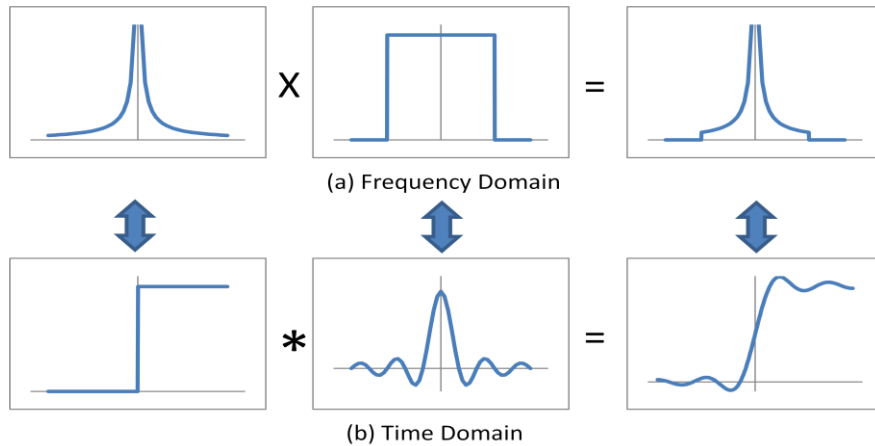


Figure 1. Multiplying the spectrum of a step function with a rectangular window produces a finite edge in the time domain

If the sweep is extended to higher frequencies – making the window function wider – the corresponding sinc pulse more closely approaches an impulse, and the time-domain edge becomes sharper. However, the oscillation never disappears for any finite sweep. Fig. 2 shows a step response for increasingly wider bandwidths.

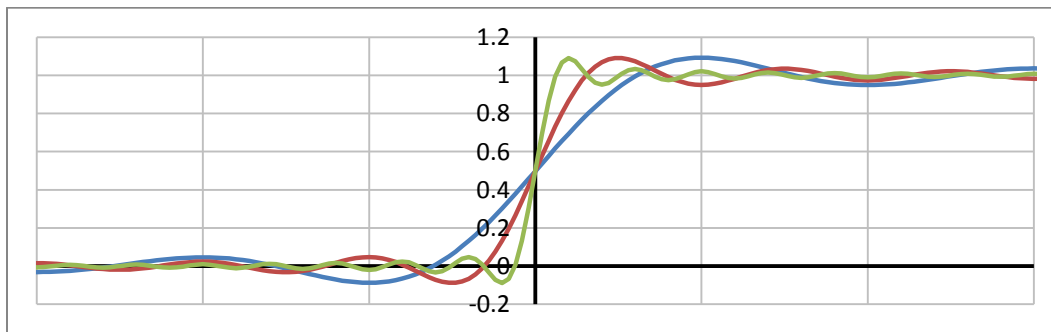


Figure 2. Increasing the width of the rectangular window makes the time-domain edge sharper, but does not eliminate the oscillation

Some distortion of the true time-domain waveform is unavoidable if the frequency sweep does not include the entire bandwidth of the signal, but there are other window functions besides the rectangle which distort the time waveform in ways which may be more desirable. In particular, it would be nice to reduce the spurious oscillation. The next sections will describe the window functions available and discuss their effects.

Window Functions

The window functions available are plotted in Figs. 3 and 4, and their expressions are given in the Appendix. All the window functions have a spectral width w and are zero-valued for $|f| > w/2$. In addition to truncating the data outside of the bandwidth, the non-rectangular windows filter the spectrum inside. The windows differ from each other in how strongly they attenuate the spectrum as the frequency approaches the upper limit. The Kaiser window has a parameter α , which controls how sharply it decays. For $\alpha = 0$, the Kaiser window is equivalent to the rectangular window; for $\alpha = 5.4414$, it is equivalent to the Hamming window; and for $\alpha = 8.885$, the Blackman window.

Although the TDR Options dialog allows for windows that are narrower than the bandwidth of the simulation, it is generally best to set the window width to 100% and take full advantage of the available bandwidth.

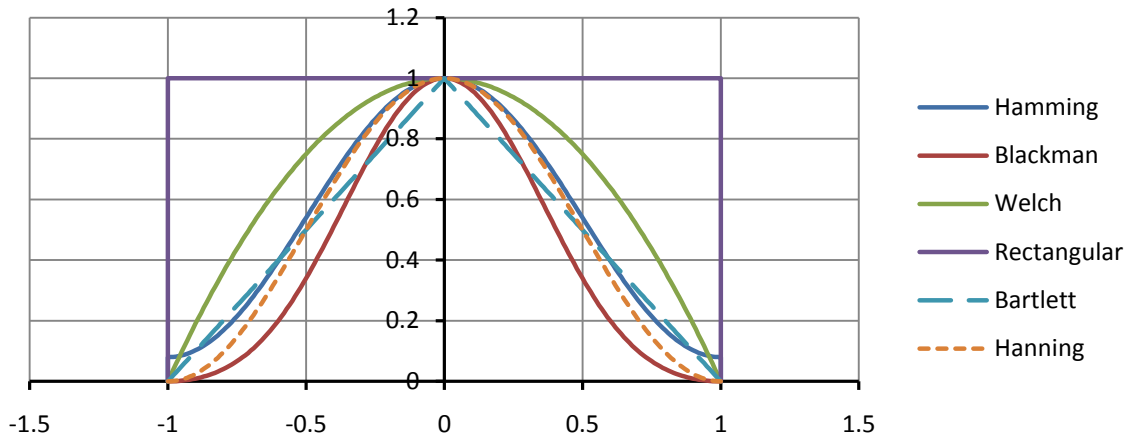


Figure 3. Window functions with a width of $w=2$

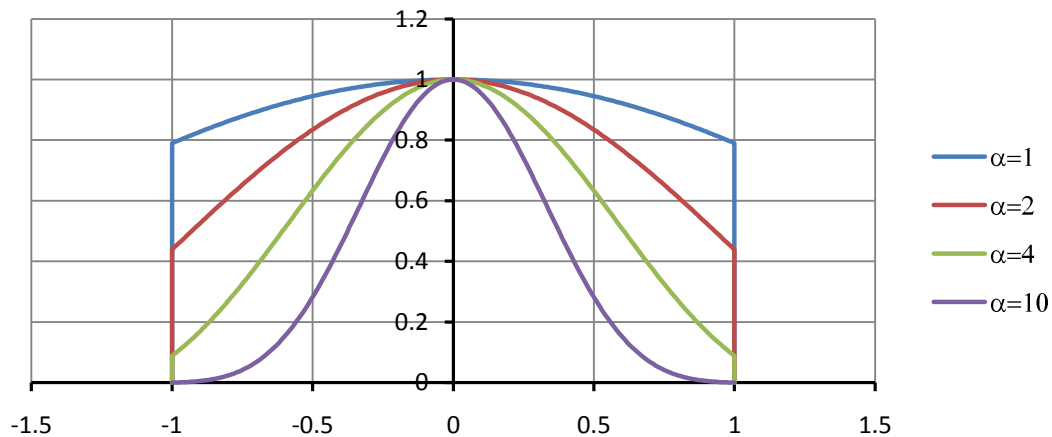


Figure 4. The Kaiser window for a width of $w=2$ and varying α values

Because the spectral width w includes both positive and negative frequencies, it is twice the bandwidth of the sweep, b , which is equal to the (positive) upper frequency limit.

Ideal Step Response

It is immaterial whether we think of the window as multiplying the frequency sweep data, with the spectrum of the time-domain excitation having infinite bandwidth, or if we instead imagine we have infinite sweep data and a windowed excitation spectrum. With the latter interpretation, we can examine the effects of different windows on an ideal step without concern for what the sweep data looks like.

We will apply different windows to an ideal step function, which is approximated in HFSS and SIwave by choosing an edge and setting the risetime to 0. We continue to assume that we have a continuous spectrum, and will defer a discussion of the effects of discretization until later. The effect of the Welch window is shown in Fig. 5.

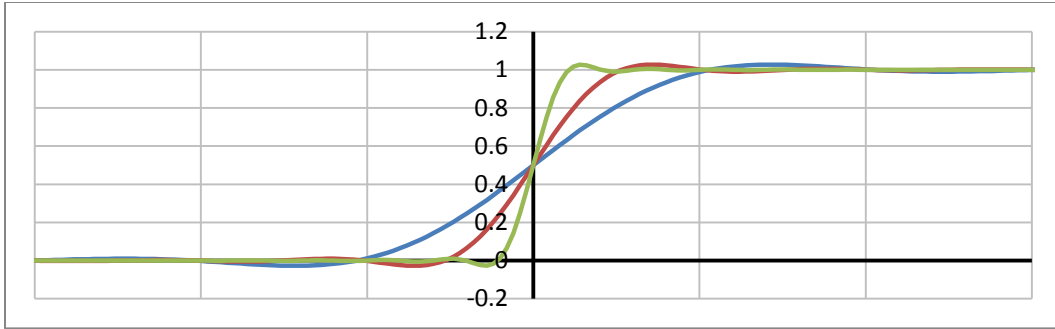


Figure 5. The effect of Welch windows of three different widths on an ideal step

Fig. 5 shows that the Welch window has substantially decreased the signal oscillation that was seen with the rectangular window. As Fig. 6 below demonstrates, the Blackman window results in almost no oscillation.

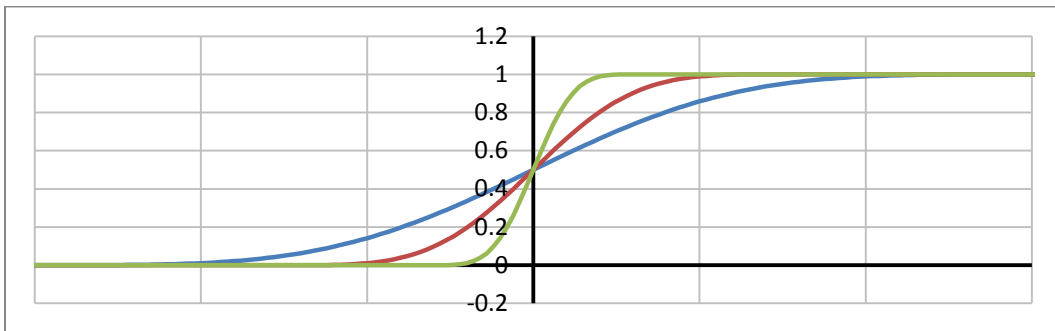


Figure 6. The effect of Blackman windows of three different widths on an ideal step

When the effects of the rectangular, Welch, and Blackman windows are plotted together, each with the same bandwidth, it is clear that there is a tradeoff between edge rate and oscillation control (Fig. 7). Windows with strong attenuation toward the frequency limits, such as the Blackman, result in minimal oscillation but slower edges. Windows with weak attenuation, such as rectangular, yield more oscillation but faster edges.

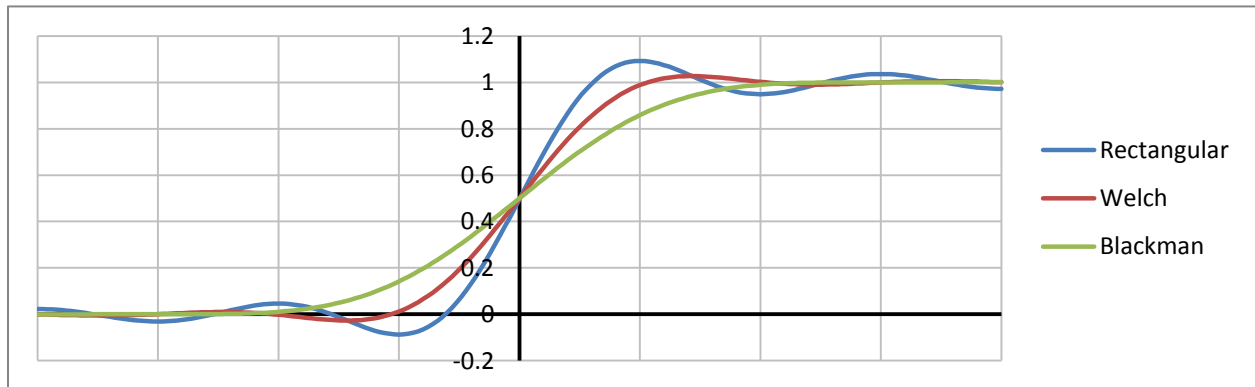


Figure 7. Step response for three different windows, each with the same bandwidth.

The effects of the Hamming, Hanning, and Bartlett windows are shown in Fig. 8 below.

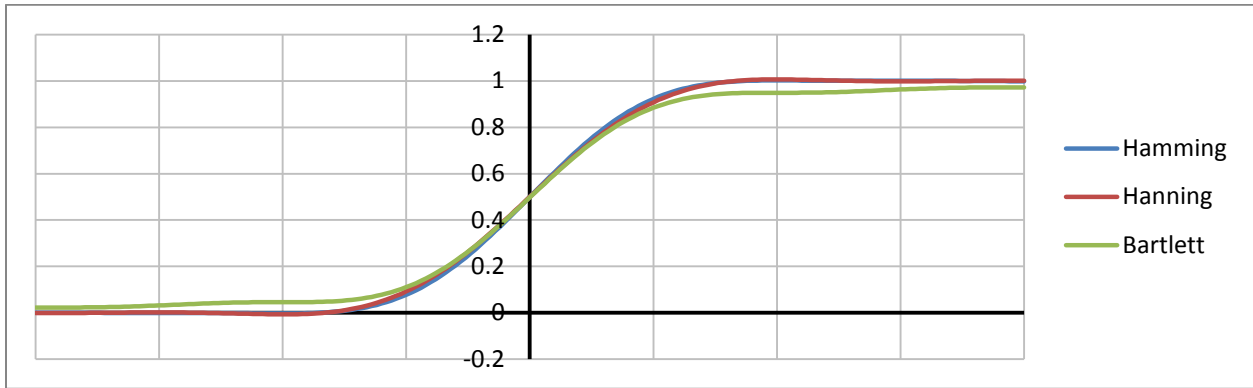


Figure 8. Hamming, Hanning, and Bartlett windows of equal bandwidth

As Fig. 8 suggests, the difference between Hamming and Hanning windows is usually quite small. The Bartlett window is generally not recommended, as it distorts the signal in the vicinity of the edge without providing any advantage over the Hamming and Hanning windows. The Kaiser window gives edges that are slower and less oscillatory with increasing α .

The rectangular, Welch, Hanning, and Blackman windows are sufficient to provide a good sampling of the edge-rate vs. oscillation tradeoff. Table 1 quantifies the characteristics of these windows on an ideal step. With the exception of the Blackman window, it is possible to derive reasonably simple expressions for the step response. In Table 1, b is the bandwidth or upper frequency limit of the sweep and $\text{Si}(x)$ refers to the sine integral function:

$$\text{Si}(x) = \int_0^x \frac{\sin z}{z} dz$$

Table 1. Characteristics of selected window functions for continuous time

Window	Step Response $f_s(t)$	10-90 Edge Rate	Max Overshoot
Rectangular	$\frac{1}{2} + \frac{\text{Si}(2\pi bt)}{\pi}$	$\frac{0.45}{b}$	8.95%
Welch	$\frac{1}{2} + \frac{\cos(2\pi bt)}{2\pi^2 bt} - \frac{\sin(2\pi bt)}{4\pi^3 b^2 t^2} + \frac{\text{Si}(2\pi bt)}{\pi}$	$\frac{0.70}{b}$	2.70%
Hanning	$\frac{2\pi + 2\text{Si}(2\pi bt) - \text{Si}(\pi - 2\pi bt) + \text{Si}(\pi + 2\pi bt)}{4\pi}$	$\frac{0.97}{b}$	0.64%
Blackman	--	$\frac{1.19}{b}$	0.02%

Note that in the expressions for the step response, the time variable is always multiplied by the bandwidth. Changing the bandwidth scales the time response, but does not affect the shape of the edge.

Finite Edge Response

Finite edges can be simulated by providing a nonzero value for the rise time. For finite edges, the same edge rate vs. oscillation tradeoff applies. However, the spectrum of a finite edge declines with frequency at a faster rate than an ideal step. As a result, modest amounts of overshoot can be achieved even with a rectangular window. The continuous-time finite edge response of a rectangular window is given by

$$f_e(t) = \frac{1}{2} - \frac{\text{Si}(2\pi b(r-t))}{\pi} + \frac{\cos(2\pi bt) - \cos(2\pi b(r-t)) + 2\pi bt (\text{Si}(2\pi b(r-t)) + \text{Si}(2\pi bt))}{2\pi^2 br}$$

The value of the edge response at $t = 0$ is given by

$$f_e(0) = \frac{1}{2} + \frac{1 - \cos(2\pi br)}{2\pi^2 br} - \frac{\text{Si}(2\pi br)}{\pi}$$

Along with the overshoot, $f_e(0)$ is a useful metric for describing how closely the finite edge response approximates the ideal case, for which $f_e(0) = 0$. The degree to which the windowed edge approximates an ideal finite edge depends only on br , the dimensionless product of the bandwidth and the rise time (Fig. 9).

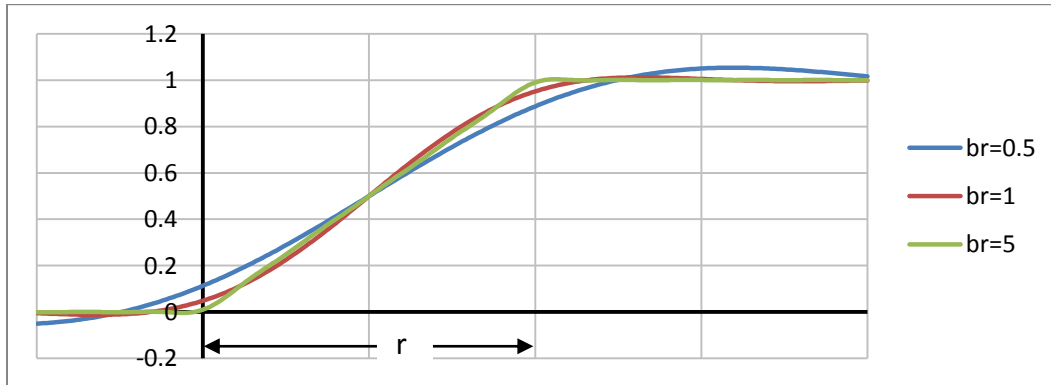


Figure 9. The effect of rectangular windows on edges with rise time r . The y-intercept and overshoot decline with increasing bandwidth b .

Table 2 below quantifies these relationships.

Table 2. Finite edge response for rectangular windows for continuous time

<i>Bandwidth*Risetime (br)</i>	<i>Edge Response at t = 0</i>	<i>Max Overshoot</i>
0.5	0.113	5.34%
0.75	0.056	2.41%
1	0.049	1.19%
2	0.025	0.72%
3	0.017	0.51%
5	0.010	0.32%
10	0.005	0.17%

As Fig. 9 and Table 2 show, a fairly good finite edge can be achieved with a br of 1, but a br of around 5 is needed to give a very close approximation to the ideal finite edge.

Impulse Response

The principles behind the step and edge responses also apply to the calculation of impulse responses. Rectangular windows produce the sharpest impulses, but with the greatest amount of oscillation. Hanning and Blackman windows produce impulses that are more spread out, but with less oscillation (Fig. 10).

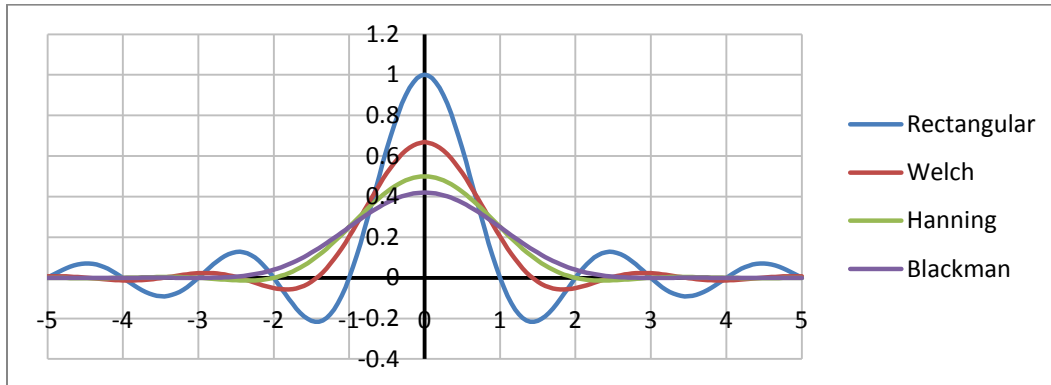


Figure 10. The impulse response for selected windows with a spectral width of 1

Discrete Time Domain Plotting

The preceding discussion treated frequency spectra as continuous functions, but in practice both the frequency and corresponding time data will be discrete. HFSS uses a discrete Fourier transform (DFT) to approximate a continuous time transform, with the frequency step size and upper limit determining the corresponding quantities in the time domain. The default time step and maximum time are given by

$$t_{step} = \frac{1}{2f_{max}} \quad t_{max} = \frac{1}{2f_{step}}$$

Time resolution is controlled by the upper frequency in the sweep. The maximum time is controlled by the frequency resolution of the sweep. While t_{max} is fixed by the choice of frequency step and cannot be increased after the simulation, t_{step} , or the time delta, can be reduced from the default value within the TDR Options Dialog. Decreasing the time delta does not increase the bandwidth of the frequency data, but it does more closely approximate the band-limited continuous time spectra we have so far discussed. Although decreasing the time delta will increase the time required to perform the DFT, the time required is rarely significant. Additionally, a smaller time delta has a significant benefit, as demonstrated in Fig. 11 below.

Fig. 11 shows the step response of a matched lossless transmission line for which the length is controlled by de-embedding the driving waveport, using rectangular window functions. The plots on the left are for a short transmission line length and those on the right correspond to a longer length. Fig. 11.a shows the time response using the default values for t_{step} . There is some oscillation in the response, which is expected for a rectangular window, but the amplitude of the oscillation is different for the two length cases. This is problematic; since the line is matched and lossless, we expect that a length change will only affect the time delay of the response, not affect the shape or quality of the rising edge. The variation in the response is an undesirable artifact of the coarse time sampling. We can increase resolution by increasing the bandwidth of the sweep, but this requires additional simulation. Fig. 11.b shows the same two cases, but with the time delta reduced using the TDR Options Dialog. The results in Fig. 11.b agree with our intuition: the edge shape is the same for both line lengths and the only

difference is the location of the edge. Setting the time delta to around 1/5 of the default value is generally sufficient, but finer timesteps are needed for precise correlation to Tables 1 and 2.

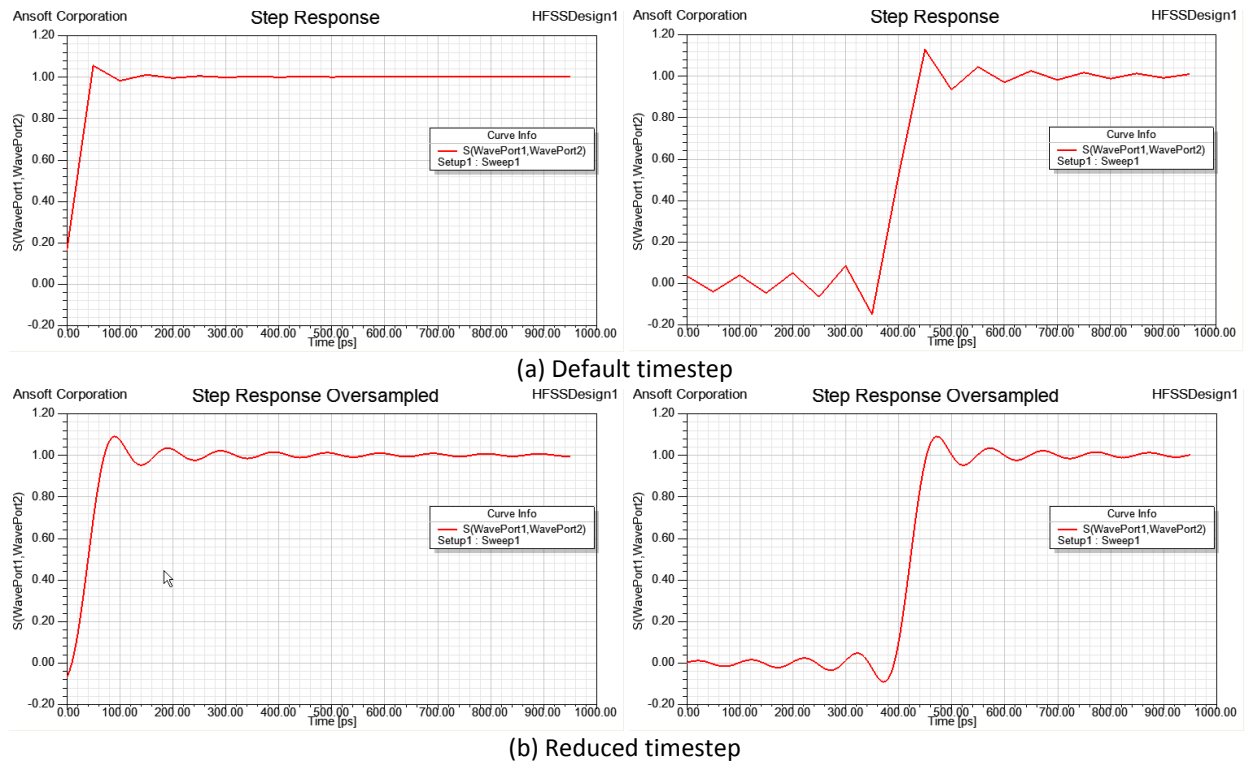


Figure 11. The time domain response of an ideal delay of two different lengths shows that a finer time sampling yields more intuitive results.

The frequency step size governs the length of the time range generated. Although a coarse frequency sampling is often sufficient to generate enough time data for a TDR plot, it is important not to set f_{step} too high in the frequency sweep. Discrete frequency spectra necessarily correspond to periodic time-domain functions, so the calculated step is actually more like a repeating series of long pulses. Fig. 12 shows the how the oscillation decays after the rising edge up to a point, but then begins increasing in anticipation of a falling edge.

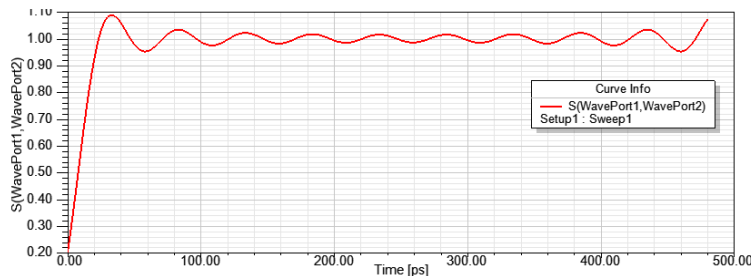


Figure 12. The oscillation caused by a rectangular window eventually starts increasing, due to the periodicity of the waveform

Setting f_{step} to a small value increases the length of the pulse, and minimizes the influence of the future falling edge. Additionally, a smaller f_{step} ensures that resonances and other sharp features in the frequency data are adequately captured. As t_{step} and f_{step} approach zero, the calculated results will converge on the continuous time descriptions given earlier.

Applications

When simulating a TDR plot, we want the fastest edge possible for the bandwidth of our simulation, subject to our preference for oscillation control. Therefore an edge with a risetime of zero is a good choice. Fig. 13 shows TDR plots of a transmission line with several impedance discontinuities. The results for a rectangular and Hanning window with a 20GHz bandwidth are compared with those for a Hanning window with a 50GHz bandwidth, which will necessarily be more accurate due to the higher bandwidth, and can be used as a reference. In all cases, the time step was set substantially lower than the default.

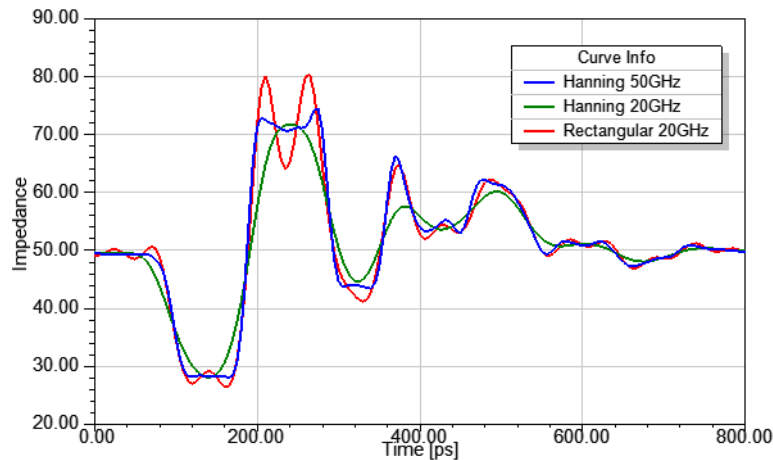


Figure 13. TDR plots for a transmission line with several impedance discontinuities

Fig. 13 shows that the rectangular window effectively captures the sharp impedance transitions, but also displays spurious oscillation. The 20GHz Hanning window does not suffer any oscillation, but gives less resolution on the sharp edges. These results are consistent with the step response characteristics of the different windows we have previously shown.

We can also use time-domain plotting to approximate how a structure would behave in a Nexxim transient simulation. When comparing the results to a transient simulation that uses a pulse or piecewise linear source, it makes sense to use a finite edge with a rectangular window. Fig. 14 compares HFSS and Nexxim results for the transmission line, using a risetime of 50ps and a rectangular window with a 20GHz bandwidth ($br = 1$).

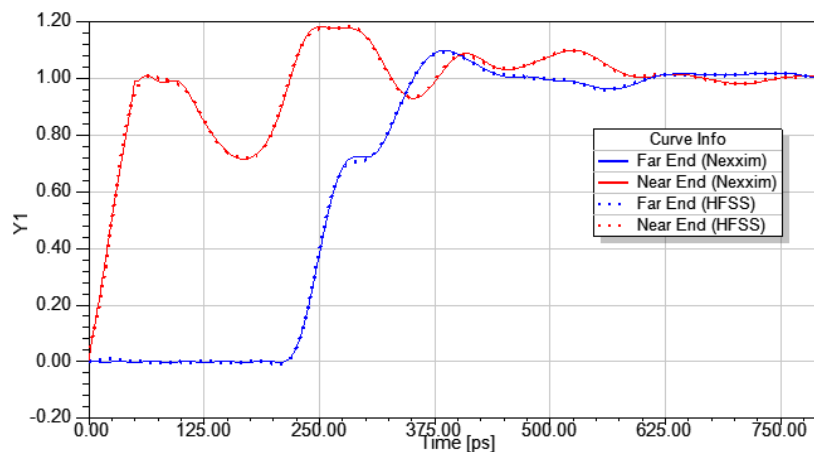


Figure 14. Waveforms at the near- and far-end of a transmission line with several impedance discontinuities, plotted with HFSS and Nexxim

As Fig. 14 shows, very good agreement between Nexxim and HFSS is possible when appropriate settings are used for time-domain plotting.

References

Haykin, S., and M. Moher. *Introduction to Analog and Digital Communications*, 2nd ed., Wiley, Hoboken, N.J., 2007.

Kammler, D.W. *A First Course in Fourier Analysis*. Prentice-Hall, Upper Saddle River, N.J., 2000.

Lathi, B.P. *Linear Systems and Signals*, 2nd ed. Oxford University Press, New York, 2005.

Appendix: Window Function Formulas

Rectangular	$\text{Rect}\left(\frac{f}{w}\right)$ where $\text{Rect}(x) = \begin{cases} 1 & -\frac{1}{2} \leq x \leq \frac{1}{2} \\ 0 & \text{otherwise} \end{cases}$
Bartlett	$1 - \left \frac{2f}{w}\right $
Blackman	$0.42 + 0.5 \cos\left(\frac{2\pi f}{w}\right) + 0.08 \cos\left(\frac{4\pi f}{w}\right)$
Hamming	$0.54 + 0.46 \cos\left(\frac{2\pi f}{w}\right)$
Hanning	$0.5 \left[1 + \cos\left(\frac{2\pi f}{w}\right)\right]$
Kaiser	$\frac{1}{I_0(\alpha)} I_0\left(\alpha \sqrt{1 - 4\left(\frac{f}{w}\right)^2}\right)$ where $I_0(x)$ is a modified Bessel function of the first kind.
Welch	$1 - \left(\frac{2f}{w}\right)^2$